

CAPITAL UNIVERSITY OF SCIENCE AND TECHNOLOGY,
ISLAMABAD



**Numerical study of MHD nanofluid flow
due to stretching permeable surface
under the effect of viscous dissipation,
Joule heating and thermal radiations**

by

Muhammad Adeel Tahir

A thesis submitted in partial fulfillment for the
degree of Master of Philosophy

in the
Faculty of Computing
Department of Mathematics

April 2017

Declaration of Authorship

I, Muhammad Adeel Tahir, declare that this thesis titled, ‘Numerical study of MHD nanofluid flow due to stretching permeable surface under the effect of viscous dissipation, joule heating and thermal radiation’ also the work mentioned in it is done by me. I also verify that:

- I have done the work wholly for a research degree at this University.
- I have clearly mentioned if any portion of the thesis is already submitted for any degree in any institution.
- If anywhere in the thesis, guidelines or help from published work of other is utilized, I have properly stated.
- Thesis is prepared according to the format of the University. It is declared that chapter 3 is review work and chapter 4 is the extension of chapter 3.
- All means of sources have been acknowledged.

Signed:

Date:

“As far as the laws of mathematics refer to reality, they are not certain, and as far as they are certain, they do not refer to reality.”

Albert Einstein

CAPITAL UNIVERSITY OF SCIENCE AND TECHNOLOGY, ISLAMABAD

Abstract

Faculty of Computing
Department of Mathematics

Master of Philosophy

by

Muhammad Adeel Tahir

The study of flow and heat transfer on a permeable stretching sheet of MHD nanofluid under the influence of convective boundary condition is presented in this dissertation. The flow is on boundary layer. The assumptions on the fluid are that it be viscous, incompressible, steady and laminar. The ordinary differential equations are obtained by applying similarity transformation on partial differential equations. Then the system is solved by using the shooting method. Software Matlab is used to compute the numerical results and the resulting values are shown through graphs and tables. Effects of viscous dissipation, Joule heating and thermal radiation are also discussed.

Acknowledgements

All appreciations are due to Allah, The Lord of the Worlds, The Most Merciful and Beneficent, who has blessed man's nature with intelligence and wisdom to search for the hidden secrets of His immense empire. Countless blessings and mercies of ALLAH may be upon Prophet Muhammad (Peace be upon him) who, by his conduct, showed us the right path.

Firstly, I thank my parents for their support and kindness. They always motivated and encouraged me during tough times in my studies. Without their prayers it was indeed impossible to successfully reach at the present stage.

I would like to express my earnest thanks and incalculable respect to my supervisor **Dr. Muhammad Sagheer** and **Dr. Shafqat Hussain**, whose sincere guidance has led me to this success. Their valuable advice, learned guidance and timely suggestions helped me to bring my dissertation into this final form and also lighted new ways to seek knowledge for me.

Finally I wish to extend my utmost thank to my friends, especially **Yasir** and **Bilal** for their constant support. Their encouragement, timely suggestions and criticism kept me inspired and moved throughout.

Contents

Declaration of Authorship	i
Abstract	iii
Acknowledgements	iv
List of Figures	vii
List of Tables	ix
Nomenclature	x
Greek Symbols	xii
1 Introduction	1
1.1 Organization of dissertation	4
2 Preliminaries	5
2.1 Basic Definitions	5
2.2 Some fundamental laws	7
2.3 Heat transfer mechanism	9
2.4 Some specific dimensionless numbers	10
3 Flow and heat transfer analysis MHD nanofluid due to convective stretching sheet	13
3.1 Introduction	13
3.2 Mathematical modeling	13
3.3 Numerical solution	16
3.4 Results and discussion	19
4 The effect of Joule heating, viscous dissipation and thermal radiation on the flow of MHD nanofluid	26
4.1 Numerical solution	28
4.2 Results and discussion	31
4.3 Conclusion	39

Bibliography**40**

List of Figures

3.1	Geometry	14
3.2	Influence of magnetic parameter on velocity profile when $N_b = N_t = Bi_1 = Bi_2 = 0.1$ and $Le = fw = 1$	21
3.3	Influence of magnetic parameter on temperature distribution when $N_b = N_t = Bi_1 = Bi_2 = 0.1$ and $Le = fw = 1$	21
3.4	Influence of magnetic parameter on concentration distribution when $N_b = N_t = Bi_1 = Bi_2 = 0.1$ and $Le = fw = 1$	22
3.5	Influence of Brownian motion parameter on temperature distribution if $N_t = Bi_1 = Bi_2 = 0.1$ and $M = Le = fw = 1$	22
3.6	Effect of thermophoresis parameter on concentration distribution when $N_b = Bi_1 = Bi_2 = 0.1$ and $M = Le = fw = 1$	22
3.7	Influence of Lewis number on concentration distribution when $N_t = N_b = Bi_1 = Bi_2 = 0.1$ and $M = fw = 1$	23
3.8	Influence of suction parameter on velocity profile when $N_b = N_t = Bi_1 = Bi_2 = 0.1$ and $Le = M = 1$	23
3.9	Influence of suction parameter on temperature distribution when $N_t = N_b = Bi_1 = Bi_2 = 0.1$ and $Le = M = 1$	23
3.10	Influence of suction parameter on concentration distribution when $N_t = N_b = Bi_1 = Bi_2 = 0.1$ and $M = Le = 1$	24
3.11	Influence of thermal Biot number on temperature distribution when $N_t = N_b = Bi_2 = 0.1$ and $Le = M = fw = 1$	24
3.12	Influence of thermal Biot number on concentration distribution when $N_t = N_b = Bi_2 = 0.1$ and $Le = M = fw = 1$	24
3.13	Influence of concentration Biot number on temperature distribution if $N_t = N_b = Bi_1 = 0.1$ and $Le = M = fw = 1$	25
3.14	Influence of concentration Biot number on concentration distribution if $N_t = N_b = Bi_1 = 0.1$ and $Le = M = fw = 1$	25
4.1	Influence of magnetic parameter on velocity profile if $E_c = N = N_b = N_t = Bi_1 = Bi_2 = 0.1$ and $Le = fw = 1$	33
4.2	Influence of magnetic parameter on temperature distribution if $N = E_c = N_b = N_t = Bi_1 = Bi_2 = 0.1$ and $Le = fw = 1$	33
4.3	Influence of magnetic parameter concentration distribution if $N = E_c = N_b = N_t = Bi_1 = Bi_2 = 0.1$ and $Le = fw = 1$	34
4.4	Influence of Brownian motion parameter on temperature distribution if $N = E_c = N_t = Bi_1 = Bi_2 = 0.1$ and $M = Le = fw = 1$	34
4.5	Influence of thermophoresis parameter on concentration distribution if $N = E_c = N_b = Bi_1 = Bi_2 = 0.1$ and $M = Le = fw = 1$	34

4.6	Influence of Lewis number on concentration distribution if $N = E_c = N_t = N_b = Bi_1 = Bi_2 = 0.1$ and $M = fw = 1$	35
4.7	Influence of suction parameter on velocity profile if $N_t = N_b = Bi_1 = Bi_2 = 0.1$ and $M = Le = 1$	35
4.8	Influence of suction parameter on temperature distribution if $N_t = N_b = Bi_1 = Bi_2 = 0.1$ and $M = Le = 1$	35
4.9	Influence of suction parameter on concentration distribution if $N_t = N_b = Bi_1 = Bi_2 = 0.1$ and $M = Le = 1$	36
4.10	Influence of thermal Biot number on temperature distribution if $N_t = N_b = Bi_2 = 0.1$ and $M = Le = fw = 1$	36
4.11	Influence of thermal Biot number on concentration distribution if $N_t = N_b = Bi_2 = 0.1$ and $M = Le = fw = 1$	36
4.12	Effect of concentration Biot number on temperature distribution when $N_t = N_b = Bi_1 = 0.1$ and $M = Le = fw = 1$	37
4.13	Effect of thermal radiation on velocity profile when $N_b = N_t = Bi_1 = Bi_2 = 0.1$ and $Le = fw = 1$	37
4.14	Effect of thermal radiation on temperature profile when $N_b = N_t = Bi_1 = Bi_2 = 0.1$ and $Le = fw = 1$	37
4.15	Effect of thermal radiation on concentration profile when $N_b = N_t = Bi_1 = Bi_2 = 0.1$ and $Le = fw = 1$	38
4.16	Effect of viscous dissipation on temperature profile when $N_b = N_t = Bi_1 = Bi_2 = 0.1$ and $Le = fw = N = 1$	38
4.17	Effect of viscous dissipation on concentration profile when $N_b = N_t = Bi_1 = Bi_2 = 0.1$ and $Le = fw = N = 1$	38

List of Tables

3.1	Comparison of results of $(-\theta'(0))$ in the absence of nanoparticles on various values of Prandtl number if $M = fw = 0$ and Bi_θ and $Bi_\phi \rightarrow \infty$	19
3.2	Numerical values of $-\theta'(0)$, $-\phi'(0)$ and $f''(0)$ for different parameters	20
4.1	Numerical values of $-f''(0)$, $-\theta'(0)$ and $-\phi'(0)$ for different parameters	32

Nomenclature

a	A real constant	Nu_x	Local Nusselt number
A^*	Space dependent heat generation	Pr	Prandtl number
B^*	Temperature dependent heat absorption	q^m	Rate of internal heat
B_0	Magnetic induction	q_w	Surface heat flux
C	Mass concentration	Re_x	Local Reynold number
C_{fx}	Skin friction in x -direction	Sh_x	Local Sherwood number
C_{fz}	Skin friction in z -direction	T	Fluid temperature
C_p	Specific heat	T_w	Fluid temperature at wall
C_w	Concentration at wall	T_∞	Ambient temperature
C_∞	Ambient concentration	(u, v, w)	Velocity vectors
D_B	Coefficient for Brownian diffusion	(x, y, z)	Axial and normal coordinates
D_T	Coefficient for Thermophoresis diffusion	α	Thermal conductivity
f	Dimensionless velocity	β_c	Concentration coefficient
g	Gravitational acceleration	β_T	Thermal expansion coefficient
Gr_c	Grashof No. for concentration difference	η	Dimensionless normal distance
Gr_x	Grashof No. for temperature difference	θ	Dimensionless temperature
h	Dimensionless transverse velocity	μ	Dynamic viscosity
h_w	Heat flux coefficient	ν	Kinematic viscosity
k	Thermal conductivity	ρ	Fluid density
Le	Lewis number	σ	Electric conductivity
m	Hall parameter	τ	Ratio of heat capacities
M	Magnetic parameter	τ_{wx}	Wall shear stress in x -direction
m_w	Surface mass flux	τ_{wz}	Wall shear stress in z -direction
Nb	Brownian motion parameter	ϕ	Dimensionless concentration
Nt	Thermophoresis parameter	ψ	Stream function

Nomenclature

Greek Symbols

Chapter 1

Introduction

The study of fluid on a stretching surface is one of the important problem discussed in the current era as it occurs in different engineering processes like extrusion, wire drawing, melt-whirling, production of glass fiber, manufacturing of rubber sheets and cooling of huge metallic plates such as an electrolyte. In the immediate surroundings of fluid the light polymer sheet composes a nonuniformly moving plane[1]. Through consecutive experiments, it is proved that the distance of the slot and velocity of stretching surface are consistent. By applying the uniform stress, the sheet bears the incompressible flow which was first studied by Crane [1]. This problem attracted other mathematicians as well, who solved this problem further by considering different physical conditions [2-5].

Nanoparticles are particles between 1 and 100 nanometers in size. Nanofluids are obtained by the dispersion of nanoparticles with basefluid. This type of fluid is from a new class of nanotechnology which is based on heat transfer. The purpose of nanofluids is to approach the maximum thermal properties at smallest possible concentration. The developments of nanofluids possess superior thermal conductivity and enhanced heat transfer characteristics. Nanofluids are homogenous mixture of nanoparticles and base fluid. Some common nanoparticles include carbons in different forms like diamond and graphite carbon nanotubes, oxide ceramics Al_2O_3 (Aluminium Oxide), CuO(Copper Oxide), metal nitrides AlN(Aluminium Nitride), SiN(Silicon Nitride), etc. All nonmetallic and metallic particles change the transport properties and heat conduction characteristics of the base fluids like water, organic liquids, e.g. ethylene, refrigerants, etc. In

fact the enhanced thermal conductivity is based on the nanoparticles while the effectiveness of heat transfer enhancement also depends upon the amount of particle shape, dispersed particles, material type, etc. The use of additives is one of the another way to enhance the heat transfer capacity of base fluids. Recent research proved that such techniques can improve the thermal conductivity and heat transport properties of the base fluid and consequently the energy efficiency. In 1995, Choi [6] made the analysis of nanoparticles and he was the first who has done work in this direction. Boungiorno et al. [7] showed the great fact that thermal conductivity of the conventional heat transfer liquids increased up to approximately two times by adding only the very small amount of nanoparticles in the fluid, that is, less than 1 by volume. Heat transport of nanofluids inside an enclosure for the solid particles dissipation was examined by Khanafer et al. [8].

Magnetohydrodynamic boundary layer stream is of great importance as it can be connected in various zones of businesses also in utilizations of geothermal. Because of its extensive variety of uses, numerous scientists have examined the attractive field impact on the liquid stream issues [9-20]. Recently, Hakeem et al. [21] concentrated the attractive field impact on second request slip stream of single stage nanofluid over an extending sheet. The connection of normal convection with thermal radiation is expanded incredibly amid the most recent decade because of its significance in numerous handy contributions. At the point when free convection streams happen at high temperature, radiation impacts on the stream get to be distinctly noteworthy. Radiation consequences for the free convection stream are critical in setting of space innovation, forms in designing ranges occurring at high temperature. In view of these applications, Olanrewaju et al. [22] examined the limit layer stream of nanofluids within the sight of radiation past a moving semi-unending level plate in a uniform free stream. Poornima et al. [23] broke down the synchronous impacts of warm radiation on warmth and mass exchange stream of nanofluids over a non-straight extending sheet. As of late, Turkyilmazoglu and Pop [24] concentrated the warm radiation impacts on the stream of single stage nanofluid over a vast vertical plate.

Viscous dissipation is quite often a negligible effect, but its contribution might become important when the fluid viscosity is very high. Rate of heat transfer is affected by the variation in temperature distribution. Anjali Devi and Ganga [25] studied the MHD

flow over a porous stretching sheet under the influence of Joule heating and viscous dissipation. Boundary layer flow along with the effects of viscous dissipation and thermal radiation over a moving flat plate were studied by Motsumi and Makinde [26]. Very recently, Makinde and Mutuku [27] investigated the thermal boundary layer of hydro-magnetic nanofluids over a heated plate under the impact of Ohmic heating and viscous dissipation. The analysis of effects of heat absorption and generation is very important in cooling processes. Although, correct displaying of internal heat generation or retention is very troublesome, some basic scientific models can express its normal conduct for most physical circumstances. Ahmed et al. [28] investigated the impacts of heat sink/source on the boundary layer flow of single phase nanofluid over a stretching tube. Very recently, Akilu and Narahari [29] studied numerically the impact of internal heat absorption of a nanofluid on natural convection flow over an inclined plate numerically.

It is important to mention here that some practical applications where the significant temperature distribution between the surface of the body and the temperature at infinity exists. The temperature distribution may cause the change in density within fluid medium or free convection due to more important existence of gravitational head. There are some circumstances where the liquid moves along with the vertical stretching sheet. In such cases, there may be some buoyancy forces due to force convection and the heat transfer distribution determined by two setups namely, the movement of stretching sheet and the gravitational effects. The thermal buoyancy is produced due to the heating/-cooling of a vertical movement of stretching sheet that becomes a large influence on the flow and heat transfer mechanism when hot fluid is moving horizontally.

Electromagnetic emissions from a surface with temperature greater than absolute zero are known as thermal radiations. These radiations can be visible, infrared or sunlight and their visibility depends on the nature of the material emitting these radiations. Since last few decades, one of the major concern in the field of science and technology is projecting source of renewable energy and this technology is mostly characterized as both active and passive solar energy. Viskant and Grosh [30] noted that these radiations become important factors when considering the cooling systems, hypersonic flights, combustion chambers and power plants.

1.1 Organization of dissertation

The main objective of this study is to review the problem of MHD nanofluid flow due to a stretching surface. Main fundamental equations attained from law of conservation of momentum and energy are then transformed into the system of coupled nonlinear ordinary differential equations by means of suitable similarity transformation and they are solved numerically by using shooting method. The same problem is discussed under the effect of viscous dissipation, Joule heating and thermal radiations and the resulting equations again are transformed by means of similarity transformation and are solved numerically by using shooting method. This dissertation is organized in following chapters.

- **Chapter 1** includes the discussion on the literature of the relevant topics.
- **Chapter 2** describes the basic ideas and terminologies which are helpful for understanding the dissertation.
- **Chapter 3** consists of review of flow and heat transfer analysis of MHD nanofluid due to convective stretching sheet.
- **Chapter 4** gives the details of the generalization of the work presented in chapter 3, under the effects of Joule heating, viscous dissipation, and thermal radiation. Conclusion and summary of the dissertation is also included in this chapter.

Chapter 2

Preliminaries

In this chapter some basic definitions, concepts and fundamental laws are described which will be useful for the understanding in the subsequent chapters.

2.1 Basic Definitions

Definition 2.1.1. (Fluid) Fluid is a substance that shows continuous deformation under the effect of shear stress.

Definition 2.1. (Fluid dynamics) The study of fluids and its characteristics at motion is known as fluid dynamics.

Definition 2.1.2. (Fluid statics) Fluid statics is that branch of fluid dynamics which focuses on the study of fluids at rest.

Definition 2.1.3. (Viscosity) When the layers of fluids try to slip by one another, the intermolecular friction is exerted which creates resistance in fluid. This frictional property of fluid is called viscosity.

Definition 2.1.4. (Dynamic viscosity) The ratio of shear stress and the rate of shear strain is called dynamic viscosity. The internal resistance of fluid is measured by dynamic viscosity.

Definition 2.1.5. (Kinematic viscosity) It is the ratio of dynamic viscosity μ and the density ρ of any base/working fluid. No force is involved in kinematic viscosity.

Mathematically it is given as

$$\nu = \frac{\mu}{\rho}.$$

Here μ represents the dynamic viscosity and ρ represents the density.

Definition 2.1.6. (Newton's law of viscosity) It states that the shear stress is comparable to the deformation rate of the fluid. Mathematically

$$\tau_{yx} = \mu \frac{du}{dy},$$

where the symbol τ_{yx} is the shear stress, x and y represents horizontal and vertical coordinates, u is the horizontal component of velocity, μ is the constant of proportionality termed as dynamic viscosity while $\frac{du}{dy}$ is the deformation rate.

Definition 2.1.7. (Newtonian fluids) All those fluids which obey the Newton's law of viscosity are known as Newtonian fluids. Gasoline and water are particular examples of Newtonian fluids.

Definition 2.1.8. (Non-Newtonian fluids) The fluids disobeying Newton's law of viscosity are called non-Newtonian fluids. Examples are toothpaste, blood, ketchup, drilling muds, biological fluids etc.. These fluids obey power law i.e.

$$\tau_{yx} = k \left(\frac{du}{dy} \right)^n,$$

where n represents the flow behaviour index and k the consistency index.

Definition 2.1.9. (Nanofluids) Nanofluids are a new technology based heat transfer fluids which are obtained by dispersing and suspending nano-particles with dimensions or order in nanometers. The purpose of the nanofluids is to achieve high thermal properties at the smallest concentration.

Definition 2.1.10. (Laminar flow) The flow where the particles of fluid move in a definite path and do not cross other's path is called laminar flow.

Definition 2.1.11. (Incompressible flow) A flow where the volume and the density of the flowing fluid remains constant is known as incompressible flow. All liquids are normally supposed to have incompressible flow.

Definition 2.1.12. (Steady flow) Steady flow is a flow where properties of fluids do not depend on time at each point in the flow. For such flows, we can write

$$\frac{d\zeta}{dt} = 0,$$

where the symbol ζ is any fluid property.

Definition 2.1.13. (Thermal conductivity) The property of the material which is related to the capacity of transmitting heat is called thermal conductivity, denoted by κ . Mathematically,

$$\kappa = \frac{q\nabla l}{S\nabla T},$$

where q is the heat passing through a surface area S and causing a temperature difference ∇T over a distance of ∇l . Here l , S and ∇T all are assumed to be of unit measurement.

Definition 2.1.14. (Thermal diffusivity) Thermal diffusivity can be defined as the ratio of thermal conductivity and density and specific heat capacity at constant pressure. It tells us that how much potential the material has for conducting thermal energy as compared to store it. Thermal diffusivity is usually denoted by α , formulated as

$$\alpha = \frac{\kappa}{\rho c_p},$$

where c_p denotes the specific heat capacity, κ the thermal conductivity and ρ the density.

2.2 Some fundamental laws

In this section, we will state the three conservation laws to obtain differential forms of the fundamental governing equations that are required in the study of different fluid flow problems.

Definition 2.2.1. (Conservation of mass) According to this law, the mass dm involved in any volume remains constant in the presence of source (place where the new matter is introduced) or sink (place where flowing matter can escape). It is stated in the mathematical form as

$$\frac{\partial \rho}{\partial t} + \nabla \cdot (\rho \vec{V}) = 0,$$

here ρ denote the density of working fluid. If the fluid is incompressible ρ becomes constant, so the equation takes the form

$$\nabla \cdot (\rho \vec{V}) = 0,$$

which gives

$$\nabla \cdot \vec{V} = 0.$$

Definition 2.2.2. (Conservation of momentum) According to the law of conservation of linear momentum when all external forces which are acting on a system balance each other, then the net momentum of the system remains constant. Mathematically,

$$\rho \frac{D\vec{V}}{Dt} = -\nabla p + \nabla \cdot \tau + \rho \vec{B},$$

where ρ , τ , p and \vec{B} is the density, Cauchy stress tensor, pressure and body force respectively. Further

$$\tau = -pI + \mu A_1,$$

$$A_1 = L + L^t,$$

$$L = \text{grad} \vec{V}.$$

For two dimension case, consider the following velocity and temperature field,

$$\vec{V} = \text{Velocity field} = [u(x, y), v(x, y), 0], \quad T = \text{temperature} = T(x, y),$$

where u and v are velocities along x and y direction respectively. As a result,

$$L = \begin{pmatrix} u_x & u_y & 0 \\ v_x & v_y & 0 \\ 0 & 0 & 0 \end{pmatrix}.$$

Definition 2.2.3. (Conservation of energy) According to the law of conservation of energy, total energy involved in a given closed system remains unchanged except the change of form. Mathematically,

$$\rho \left[\frac{\partial h}{\partial t} + \nabla \cdot (h \vec{V}) \right] = \frac{Dp}{Dt} + \nabla \cdot (k \nabla T) + \hat{\phi},$$

where ρ , τ , p , ∇T and $\hat{\phi}$ is the density, specific enthalpy, temperature gradient and dissipation function, respectively.

2.3 Heat transfer mechanism

Due to internal forces, heat transfer from higher temperature to the low temperature. Heat transfer may occur in the following ways.

Definition 2.3.1. (Conduction) The transfer of heat from one body to another body that are in direct contact with each other is called conduction.

Definition 2.3.2. (Convection) Convection is that mechanism of heat transfer which includes changing location of molecules with time. This change in position causes a higher temperature difference and higher rate of heat flux. There are three types of convection.

(i) Forced convection

Forced convection is a heat transfer mechanism in which fan or pump or any other device which acts as an outer source disturbs the fluid motion.

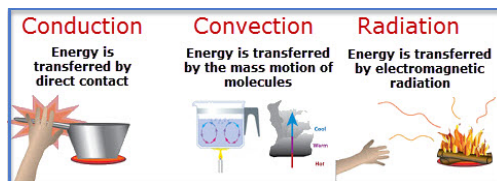
(ii) Natural convection

Natural convection also termed as free convection flow field is self continued flow caused by the existence of temperature difference. The density and the buoyancy of the fluid is affected by this convection. Natural convection occurs by the action of density gradients in conjunction with a gravitational field. It is also called an buoyant convection.

(iii) Mixed convection

Mixed convection is a combination of both forced and free convection. For example, if fluid is moving vertically upward along the moment of the vertical stretching sheet is forced convection while in the same phenomena fluid is freely falling due to the gravity which is free convection. When these two phenomena appear in the same model then such kind of flow is mixed convection.

Definition 2.3.3. (Radiation) Radiation is the emission of energy in the form of waves or particles.



Definition 2.3.4. (Boundary layer) Boundary layer is a flow layer of fluid close to the solid region of the wall in contact where the viscosity effects are significant. The flow in this layer is usually laminar. The boundary layer thickness is the measure of the distance apart from the surface.

2.4 Some specific dimensionless numbers

In this section we will define some dimensionless numbers used in subsequent chapters.

(i) Prandtl number

Prandtl number gives the quantitative relation between the momentum diffusion rate and thermal diffusion rate. Mathematically, it is defined as:

$$Pr = \frac{\nu}{\alpha} = \frac{\frac{\mu}{\rho}}{\frac{\kappa}{\rho c_p}} = \frac{\mu c_p}{\kappa},$$

where the kinematic viscosity or momentum diffusivity is denoted by ν and the thermal diffusivity is denoted by α . It gives the comparative thickness of velocity and the domain of thermal boundary layers. For very very small values of Pr heat diffuses rapidly as compared to the inertial force.

(ii) Nusselt number

It is defined as the ratio between transfer of heat by convection and heat transport by conduction in the direction normal to the boundary. Mathematically,

$$Nu_x = \frac{\text{convective heat transfer coefficient}}{\text{conductive heat transfer coefficient}}$$

$$Nu_x = \frac{h \nabla T}{\frac{\kappa \nabla T}{L}} = \frac{hL}{\kappa}.$$

Here $h \nabla T$ represents heat transfer by convection, $\frac{\kappa \nabla T}{L}$ the heat transfer by conduction, h the convective heat transfer, L the characteristic length and κ the thermal conductivity of fluid.

(iii) Biot number

We know that resistance of heat transfer is different inside of the material and at the surface. Their ratio is called Biot number. Mathematically it is defined as

$$Bi = \frac{hL}{\kappa},$$

here h is convective heat transfer, L represents the characteristic length and κ the thermal conductivity of the fluid.

(iii) Lewis number

The Lewis number can be defined as the ratio of thermal diffusivity with molecular diffusivity. It helps us to find the relationship between mass and heat transfer coefficient. Mathematically,

$$Le = \frac{\lambda}{\rho D_m c_p},$$

where λ is the convective heat transfer coefficient, D_m the mixture-averaged diffusion coefficient, and c_p the specific heat capacity at constant pressure.

(iv) Brownian diffusion coefficient

Brownian diffusion occurs due to continuous collision between the molecules and nanoparticle of the fluid. The Brownian diffusion coefficient D_B is given by

$$D_B = \frac{K_B T C_c}{3\pi\mu d_p},$$

where K_b, T, C_c and μ represents Boltzmann constant, temperature, correction factor and viscosity respectively.

(v) Thermophoretic diffusion coefficient

Thermophoresis diffusion occurs when particles diffuse due to the effect of temperature gradient. The thermophoretic diffusion coefficient is given by

$$D_T = \frac{-v_{th}T}{\nu\nabla T},$$

where v_{th}, T, ν and ∇T denote thermophoretic velocity, temperature, kinematic viscosity and temperature gradient respectively.

(vi) Skin friction coefficient

Skin friction coefficient represents the value of friction which occurs when fluid

moves across the surface. Mathematically

$$C_f = \frac{2T_{yx}}{\rho U_e^2}$$

where T_{yx} is the shear stress at the wall, ρ the density and U_e the free-stream velocity.

(vii) Sherwood Number

It is the nondimensional quantity which show the ratio of the mass transport by convection to the transfer of mass by diffusion. Mathematically

$$Sh_x = \frac{kL}{D}$$

here L is characteristic length, D is the mass diffusivity and k is the mass transfer coefficient.

Definition 2.4.1. (Similarity transformation) Similarity transformation is a tool used in mathematics, which helps us to transform the partial differential equations, which occurs in a problem, into the system of coupled ordinary differential equations (ODEs). The technique reduces a number of independent variables of the problem. It can be stated in a way that it is a rule which combines the two independent variable to get a new one.

Definition 2.4.2. (Viscous dissipation) The process in which the work done by fluid in converted into heat is called viscous dissipation. It is an irreversible process,

Definition 2.4.3. (Thermal radiation) The ejection of electromagnetic waves from the matters that have temperature higher than absolute zero is called thermal radiation.

Definition 2.4.4. (Joule heating) The heat which is produced due to flow of current through conductor is called Joule heating.

Chapter 3

Flow and heat transfer analysis MHD nanofluid due to convective stretching sheet

3.1 Introduction

In the present chapter, we have reviewed [31] the MHD nanofluid flow at a boundary layer over a stretching surface placed vertically. As discussed in [31], we have assumed that fluid is steady, laminar and incompressible. By stretching the sheet linearly in the x -direction by fixing the origin, the flow is generated. The nonlinear coupled ordinary differential equations (ODEs) are obtained after converting the system of partial differential equations by applying the similarity transformation. These equations are numerically solved with the help of shooting method. Results are obtained for each physical parameter involved in the equations.

3.2 Mathematical modeling

Consider a steady flow of an incompressible nanofluid in the region $y > 0$ induced by a permeable stretching surface located at $y = 0$ with a fixed origin at $x = 0$ as displayed in figure (3.1). From the slot at the origin thin solid surface is extruded which is being stretched in x -direction. The stretching velocity $u_w(x) = cx$ is assumed to vary linearly

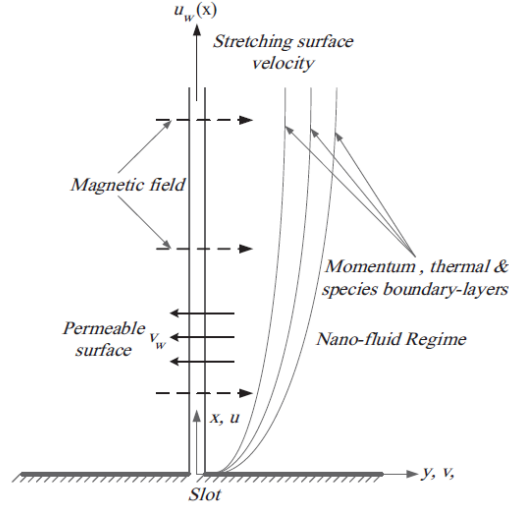


FIGURE 3.1: Geometry

from the origin, where c is a positive constant ($c > 0$). It is also assumed that the temperature and nanofluid volume fraction at the surface of the sheet are respectively T_w and C_w , while the uniform temperature and the nanofluid volume fraction far from the surface of the sheet are T_∞ and C_∞ , respectively. The magnetic field of strength B_0 is applied perpendicular to the stretching sheet. The flow is described by the equation of continuity, equation of momentum and energy equation as

$$\frac{\partial u}{\partial x} + \frac{\partial v}{\partial y} = 0, \quad (3.1)$$

$$u \frac{\partial u}{\partial x} + v \frac{\partial u}{\partial y} = \nu \frac{\partial^2 u}{\partial y^2} - \sigma \frac{B_0^2}{\rho} u, \quad (3.2)$$

$$u \frac{\partial T}{\partial x} + v \frac{\partial T}{\partial y} = \alpha \left(\frac{\partial^2 T}{\partial y^2} \right) + \tau \left[D_B \left(\frac{\partial C}{\partial y} \frac{\partial T}{\partial y} \right) + \frac{D_T}{T_\infty} \left(\frac{\partial T}{\partial y} \right)^2 \right], \quad (3.3)$$

$$u \frac{\partial C}{\partial x} + v \frac{\partial C}{\partial y} = D_B \left(\frac{\partial^2 C}{\partial y^2} \right) + \frac{D_T}{T_\infty} \left(\frac{\partial T}{\partial y} \right)^2. \quad (3.4)$$

where $\nu = \frac{\mu}{\rho}$ is the kinematic viscosity, ρ is the fluid density, σ is the electrical conductivity, B_0 is the magnetic field imposed along y-axis, T represents the temperature of fluid, α is the thermal diffusivity, c_p the specific heat capacity of the nanoparticle material, C the nanoparticle fluid concentration, D_B represents the Brownian diffusion coefficient, and D_T is the thermophoretic diffusion coefficient. The perpendicular and parallel coordinates to the surface are y and x , the components of velocity are u and v

in the direction of x and y . Boundary conditions can be written as

$$u = u_w(x), v = v_x, -K \frac{\partial T}{\partial y} = h_1(T_w - T), -D_B \frac{\partial C}{\partial y} = h_2(C_w - C) \quad \text{at } y = 0, \quad (3.5)$$

$$u \rightarrow 0, \quad T \rightarrow T_\infty, C \rightarrow C_\infty \quad \text{as } y \rightarrow \infty \quad (3.6)$$

In the above equations, T is fluid temperature, T_∞ the surrounding temperature, h_s the heat transfer coefficient, ν is the kinematic viscosity and α the thermal diffusivity. The equation of continuity can be justified if a stream function ψ is chosen in a way that

$$u = \frac{\partial \psi}{\partial y} \quad \text{and} \quad v = -\frac{\partial \psi}{\partial x}.$$

Introduce the following similarity transformation,

$$\psi = (av)^{\frac{1}{2}} x f(\eta), \quad \eta = \left(\frac{a}{v} \right)^{\frac{1}{2}} y,$$

$$\theta(\eta) = \frac{T - T_\infty}{T_w - T_\infty},$$

$$\theta(\eta) = \frac{C - C_\infty}{C_w - C_\infty}.$$

By introducing the similarity transformation defined as above, equations (3.2) – (3.4) becomes

$$f''' + ff'' - (f')^2 - Mf' = 0, \quad (3.7)$$

$$\theta'' + Pr[f\theta' + Nb\theta'\phi' + Nt(\theta')^2] = 0 \quad (3.8)$$

$$\theta'' + Le\theta' + \frac{Nt}{Nb}\theta'' = 0 \quad (3.9)$$

where

$$M = \frac{\sigma B_0^2}{\rho a}, \quad Pr = \frac{\nu}{\alpha}, \quad Nb = \tau D_B \frac{(C_w - C_\infty)}{\nu},$$

$$Nt = \tau D_T \frac{(T_w - T_\infty)}{\nu T_\infty} \quad \text{and} \quad Le = \frac{\alpha}{D_B}$$

The associated boundary conditions (3.5) and (3.6) get the form,

$$f(0) = f_w \quad f'(0) = 1, \quad \theta'(0) = -B_{i_\theta}(1 - \theta(0)), \quad \phi'(0) = -B_{i_\phi}(1 - \phi(0)), \quad (3.10)$$

$$\theta \rightarrow 0, \quad \phi \rightarrow 0 \quad \text{when } \eta \rightarrow \infty \quad (3.11)$$

3.3 Numerical solution

In order to solve the above obtained ODEs, we have used the shooting method. To solve the above system numerically, we have replaced the domain $[0, \infty)$ by the bounded domain $[0, \eta_\infty]$ where η_∞ is some suitable finite real number. Let us use the notation $f = y_1$, $\theta = y_4$, $\phi = y_6$. Further denote $f' = y_1'$ by y_2 , $f'' = y_2'$ by y_3 , θ' by y_5 , $\phi' = y_6'$ by y_7 to have the following system of first order ODEs.

$$y_1' = y_2, \quad y_1(0) = f_w \quad (3.12)$$

$$y_2' = y_3, \quad y_2(0) = 1 \quad (3.13)$$

$$y_3' = y_2^2 + My_2 - y_1y_3, \quad y_3(0) = Y_3 \quad (3.14)$$

$$y_4' = y_5, \quad y_4(0) = Y_4 \quad (3.15)$$

$$y_5' = -Pr(y_1y_5 + N_b y_5 y_7 + N_t y_7^2), \quad y_5(0) = -B_{i_\theta}(1 - t) \quad (3.16)$$

$$y_6' = y_7, \quad y_6(0) = Y_6 \quad (3.17)$$

$$y_7' = \frac{N_t}{N_b} Pr(y_1y_5 + N_b y_5 y_7 + N_t y_7^2) - L_c y_1 y_7, \quad y_7(0) = -B_{i_\phi}(1 - u). \quad (3.18)$$

In the system of equations (3.12) – (3.18), the missing initial conditions Y_3 , Y_4 and Y_6 are to be chosen such that

$$y_2(\eta_\infty, Y_3, Y_4, Y_6) = 0, \quad y_4(\eta_\infty, Y_3, Y_4, Y_6) = 0, \quad y_6(\eta_\infty, Y_3, Y_4, Y_6) = 0. \quad (3.19)$$

To solve the system of algebraic equations (3.19), we use the Newton's method which has the following iterative scheme

$$\begin{pmatrix} Y_3^{(k+1)} \\ Y_4^{(k+1)} \\ Y_6^{(k+1)} \end{pmatrix} = \begin{pmatrix} Y_3^{(k)} \\ Y_4^{(k)} \\ Y_6^{(k)} \end{pmatrix} - \begin{pmatrix} \frac{\partial y_2}{\partial Y_3} & \frac{\partial y_2}{\partial Y_4} & \frac{\partial y_2}{\partial Y_6} \\ \frac{\partial y_4}{\partial Y_3} & \frac{\partial y_4}{\partial Y_4} & \frac{\partial y_4}{\partial Y_6} \\ \frac{\partial y_6}{\partial Y_3} & \frac{\partial y_6}{\partial Y_4} & \frac{\partial y_6}{\partial Y_6} \end{pmatrix}_{(\eta_\infty, Y_3^{(k)}, Y_4^{(k)}, Y_6^{(k)})}^{-1} \begin{pmatrix} y_2^{(k)} \\ y_4^{(k)} \\ y_6^{(k)} \end{pmatrix}_{(Y_3^{(k)}, Y_4^{(k)}, Y_6^{(k)})}.$$

Let us now use the following notations:

$$\begin{aligned} \frac{\partial y_1}{\partial Y_3} &= y_8, \quad \frac{\partial y_2}{\partial Y_3} = y_9, \quad \dots \quad \frac{\partial y_7}{\partial Y_3} = y_{14}, \\ \frac{\partial y_1}{\partial Y_4} &= y_{15}, \quad \frac{\partial y_2}{\partial Y_4} = y_{16}, \quad \dots \quad \frac{\partial y_7}{\partial Y_4} = y_{21}, \\ \frac{\partial y_1}{\partial Y_6} &= y_{22}, \quad \frac{\partial y_2}{\partial Y_6} = y_{23}, \quad \dots \quad \frac{\partial y_7}{\partial Y_6} = y_{28}. \end{aligned}$$

With these new notation, the Newton's iterative scheme get the following form.

$$\begin{pmatrix} Y_3^{(k+1)} \\ Y_4^{(k+1)} \\ Y_6^{(k+1)} \end{pmatrix} = \begin{pmatrix} Y_3^{(k)} \\ Y_4^{(k)} \\ Y_6^{(k)} \end{pmatrix} - \begin{pmatrix} y_9 & y_{16} & y_{23} \\ y_{11} & y_{18} & y_{25} \\ y_{13} & y_{20} & y_{27} \end{pmatrix}_{(\eta_\infty, Y_3^{(k)}, Y_4^{(k)}, Y_6^{(k)})}^{-1} \begin{pmatrix} y_2^{(k)} \\ y_4^{(k)} \\ y_6^{(k)} \end{pmatrix}_{(Y_3^{(k)}, Y_4^{(k)}, Y_6^{(k)})} \quad (3.20)$$

For the execution of the above iterative scheme, we differentiate equations (3.12) – (3.18) with respect to each variable $Y_3, Y_4,$ and Y_6 to have the following IVP consisting of system of twenty one ODEs:

$$y'_8 = y_9, \quad y_8(0) = 0 \quad (3.21)$$

$$y'_9 = y_{10}, \quad y_9(0) = 0 \quad (3.22)$$

$$y'_{10} = 2y_2y_9 + My_9 - [y_8y_3 + y_1y_{10}], \quad y_{10}(0) = 1 \quad (3.23)$$

$$y'_{11} = y_{12}, \quad y_{11}(0) = 0 \quad (3.24)$$

$$y'_{12} = -P_r[y_8y_5 + y_1y_{12} + N_b(y_{12}y_7 + y_5y_{14}) + 2N_t y_7 y_{14}], \quad y_{12}(0) = 0 \quad (3.25)$$

$$y'_{13} = y_{14}, \quad y_{13}(0) = 0 \quad (3.26)$$

$$y'_{14} = \frac{N_t}{N_b} P_r[(y_8y_5 + y_1y_{12}) + N_b(y_{12}y_7 + y_5y_{14}) + 2N_t y_7 y_{14}] \\ - L_e(y_8y_7 + y_1y_{14}), \quad y_{14}(0) = 0 \quad (3.27)$$

$$y'_{15} = y_{16}, \quad y_{15}(0) = 0 \quad (3.28)$$

$$y'_{16} = y_{17}, \quad y_{16}(0) = 0 \quad (3.29)$$

$$y'_{17} = 2y_2y_{16} + My_{16} - [y_{15}y_3 + y_1y_{17}], \quad y_{17}(0) = 0 \quad (3.30)$$

$$y'_{18} = y_{19}, \quad y_{18}(0) = 1 \quad (3.31)$$

$$y'_{19} = -P_r[y_{15}y_5 + y_1y_{19} + N_b(y_{19}y_7 + y_5y_{21}) + 2N_t y_7 y_{21}], \quad y_{19}(0) = -B_{i_\theta} \quad (3.32)$$

$$y'_{20} = y_{21}, \quad y_{20}(0) = 0 \quad (3.33)$$

$$y'_{21} = \frac{N_t}{N_b} P_r[(y_{15}y_5 + y_1y_{19}) + N_b(y_{19}y_7 + y_5y_{21}) + 2N_t y_7 y_{21}] \\ - L_e(y_{15}y_7 + y_1y_{21}), \quad y_{21}(0) = 0 \quad (3.34)$$

$$y'_{22} = y_{23}, \quad y_{22}(0) = 0 \quad (3.35)$$

$$y'_{23} = y_{24}, \quad y_{23}(0) = 0 \quad (3.36)$$

$$y'_{24} = 2y_2y_{23} + My_{23} - [y_{22}y_3 + y_1y_{24}], \quad y_{24}(0) = 0 \quad (3.37)$$

$$y'_{25} = y_{26}, \quad y_{25}(0) = 0 \quad (3.38)$$

$$y'_{26} = -P_r[y_{22}y_5 + y_1y_{26} + N_b(y_{26}y_7 + y_5y_{28}) + 2N_t y_7 y_{28}], \quad y_{26}(0) = 0 \quad (3.39)$$

$$y'_{27} = y_{28}, \quad y_{27}(0) = 1 \quad (3.40)$$

$$y'_{28} = \frac{N_t}{N_b} P_r[(y_{22}y_5 + y_1y_{26}) + N_b(y_{26}y_7 + y_5y_{28}) + 2N_t y_7 y_{28}] \\ - L_e(y_{22}y_7 + y_1y_{28}), \quad y_{28}(0) = -B_{i_\phi}. \quad (3.41)$$

The above equations are solved using Runge-Kutta method of order 4 with an initial

guess $Y_3^{(0)}, Y_4^{(0)}, Y_6^{(o)}$. These guesses are updated by the Newton's method. The iterative process is repeated until the following criteria is met

$$\max(|y_2(\eta_\infty) - |, |y_4(\eta_\infty) - |, |y_6(\eta_\infty) - |) < \epsilon,$$

where $\epsilon > 0$ is the tolerance. For all computation in this chapter, we have fixed $\epsilon = 10^{-8}$. The results are compared with [32-35] and we concluded that results are acceptable.

3.4 Results and discussion

Table 3.1 shows the comparison of calculated values with [32-35] and strong agreement with the values is found which showed high confidence of present simulation. From table it is observed that Nusselt number is increased by increase of Prandtl number. Table 3.2 shows the skin-friction coefficient ($-f''(0)$) increases by the increase of M. The effect of M on Nusselt number ($-\theta'(0)$) and Sherwood number ($-\phi'(0)$) is opposite as compared to skin-friction coefficient. The magnitude of skin-friction coefficient also increases by increasing the suction parameter. Sherwood number increases by increasing Lewis number. Effects of thermal and concentration Biot number are similar.

Pr	[32]	[33]	[34]	[35]	Current values
0.70	0.4539	0.5349	0.4539	0.4539	0.4539
2.00	0.9114	0.9114	0.9113	0.9114	0.9114
7.00	1.8954	1.8905	1.8954	1.8954	1.8954

TABLE 3.1: Comparison of results of $(-\theta'(0))$ in the absence of nanoparticles on various values of Prandtl number if $M = fw = 0$ and Bi_θ and $Bi_\phi \rightarrow \infty$

Figures 3.1, 3.2 and 3.3 show the effect of magnetic parameter on velocity profile, temperature distribution and concentration distribution respectively. It can be seen from the figures that thickness of velocity boundary layer is decreased by the increase of magnetic parameter whereas temperature and concentration distribution show a little increase with the increase in magnetic parameter. It is due to the Lorentz force which is created by applying magnetic field to the conducting fluid. Lorentz force has the capacity to reduce the speed of flow which supports our results. By applying magnetic field on the fluid, the resistance on the fluid particles increases which results in the increase in temperature. Figures 3.4 and 3.5 represent the effect of Brownian motion

M	Le	f_w	N_t	N_b	Bi_1	Bi_2	$-f''(0)$	$-\theta'(0)$	$-\phi'(0)$
0	1	1	0.1	0.1	0.1	0.1	1.076829	0.236852	0.337043
1							1.276822	0.226852	0.321234
2							1.364217	0.216854	0.317043
3							1.442316	0.202315	0.306044
1	1	1	0.1	0.1	0.1	0.1	1.076859	0.236855	0.307041
				0.3			1.076859	0.236855	0.307041
				0.5			1.076858	0.236855	0.307042
				0.7			1.076858	0.236854	0.307042
			0.1	0.1			1.076859	0.236854	0.307042
			0.3				1.176761	0.236859	0.307048
			0.5				1.266862	0.236860	0.307048
			0.7				1.396865	0.236861	0.307049
1	1	1	0.1	0.1	0.1	0.1	1.076862	0.236861	0.307049
	2						1.176853	0.246862	0.317051
	3						1.257686	0.256871	0.325052
	4						1.346869	0.266846	0.332054
1	1	0	0.1	0.1	0.1	0.1	1.076862	0.236864	0.307055
		1					1.176565	0.236861	0.307055
		2					1.276590	0.236859	0.307053
		3					1.366558	0.236858	0.307051
1	1	1	0.1	0.1	0.1	0.1	1.076561	0.236561	0.307053
					0.3		1.076563	0.236563	0.307055
					0.5		1.076564	0.236564	0.307056
					0.7		1.076565	0.236565	0.307058
1	1	1	0.1	0.1	0.1	0.1	1.076566	0.236567	0.307059
						0.3	1.076568	0.236568	0.307063
						0.5	1.076569	0.236569	0.307065
						0.7	1.076572	0.236569	0.307069

TABLE 3.2: Numerical values of $-\theta'(0)$, $-\phi'(0)$ and $f''(0)$ for different parameters

parameter and thermophoresis parameter on the profiles of temperature and concentration. An increase in Brownian motion parameter increase the temperature. Similarly by increasing thermophoresis parameter increase in the concentration distribution is seen. So distribution of nano particles can be adjusted by adjusting Brownian motion parameter. It can also be said that thermophoresis helps in diffusion of nano particles. Figure 3.6 reflects the effect of Lewis number on concentration profile. Lewis number can be defined as the ratio of thermal diffusion to the molecular diffusion. It is convenient of help us find the relation between mass and heat transfer coefficient. By increasing Lewis number the concentration profile becomes more steeper. Figures 3.7, 3.8 and 3.9 represent the effect of suction parameter on velocity profile, temperature distribution and concentration distribution. By increasing the suction parameter a decrease in velocity profile, temperature distribution and concentration distribution is observed. If suction

is applied on vertical surface it allows the fluid to draw in the surface which affects the boundary layer thickness. Figures 3.10, 3.11, 3.12 and 3.13 represent the effect of thermal Biot number and concentration Biot number on temperature and concentration distribution. Increase in thermal and concentration Biot number increases the temperature and concentration distribution. Increase in Biot numbers, increases heat transfer coefficient which increases the temperature.

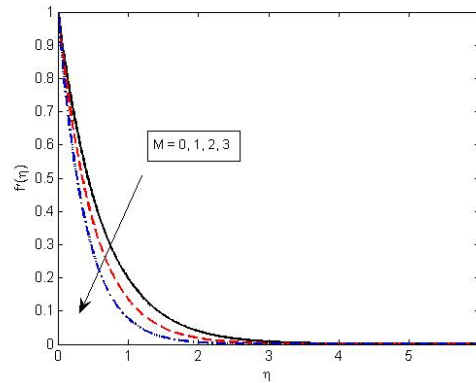


FIGURE 3.2: Influence of magnetic parameter on velocity profile when $N_b = N_t = Bi_1 = Bi_2 = 0.1$ and $Le = fw = 1$

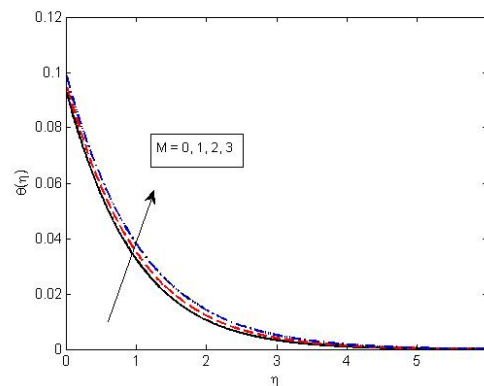


FIGURE 3.3: Influence of magnetic parameter on temperature distribution when $N_b = N_t = Bi_1 = Bi_2 = 0.1$ and $Le = fw = 1$

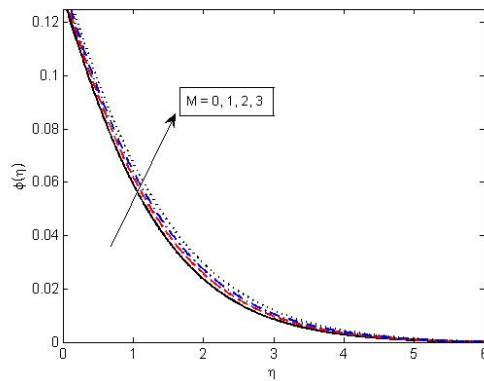


FIGURE 3.4: Influence of magnetic parameter on concentration distribution when $N_b = N_t = Bi_1 = Bi_2 = 0.1$ and $Le = fw = 1$

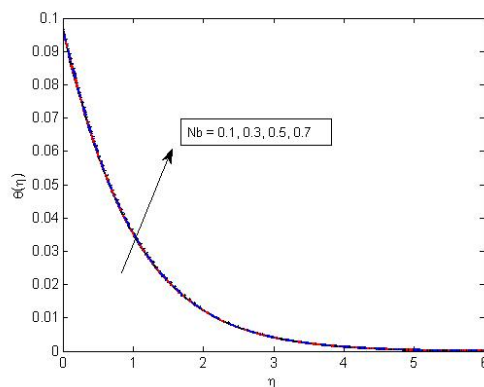


FIGURE 3.5: Influence of Brownian motion parameter on temperature distribution if $N_t = Bi_1 = Bi_2 = 0.1$ and $M = Le = fw = 1$

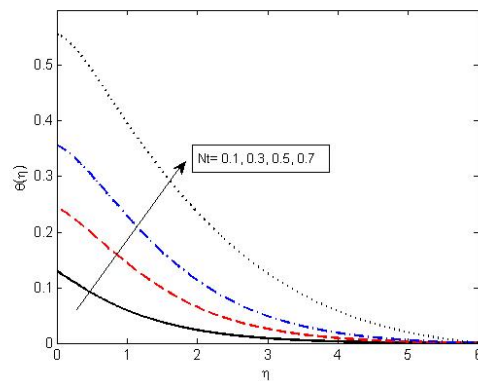


FIGURE 3.6: Effect of thermophoresis parameter on concentration distribution when $N_b = Bi_1 = Bi_2 = 0.1$ and $M = Le = fw = 1$

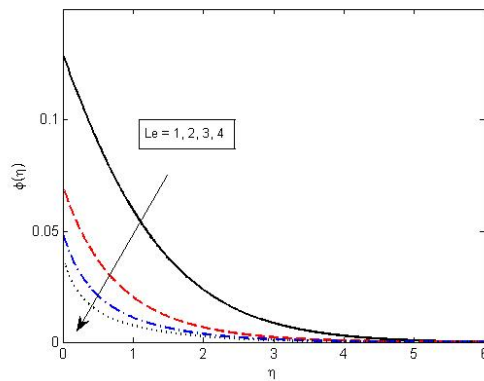


FIGURE 3.7: Influence of Lewis number on concentration distribution when $N_t = N_b = Bi_1 = Bi_2 = 0.1$ and $M = fw = 1$

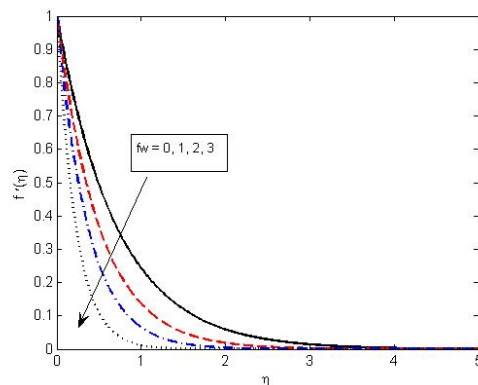


FIGURE 3.8: Influence of suction parameter on velocity profile when $N_b = N_t = Bi_1 = Bi_2 = 0.1$ and $Le = M = 1$

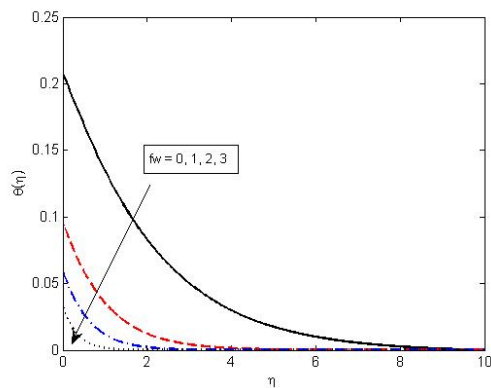


FIGURE 3.9: Influence of suction parameter on temperature distribution when $N_t = N_b = Bi_1 = Bi_2 = 0.1$ and $Le = M = 1$

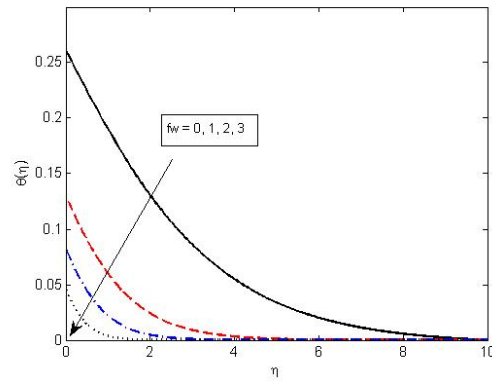


FIGURE 3.10: Influence of suction parameter on concentration distribution when $N_t = N_b = Bi_1 = Bi_2 = 0.1$ and $M = Le = 1$

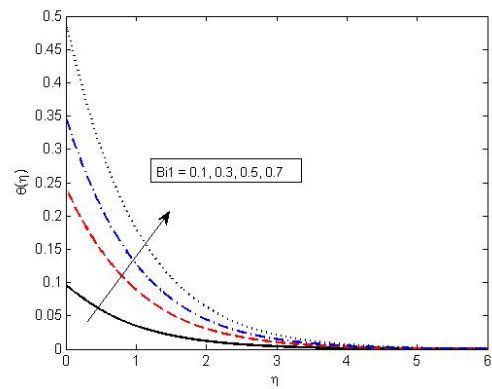


FIGURE 3.11: Influence of thermal Biot number on temperature distribution when $N_t = N_b = Bi_2 = 0.1$ and $Le = M = fw = 1$

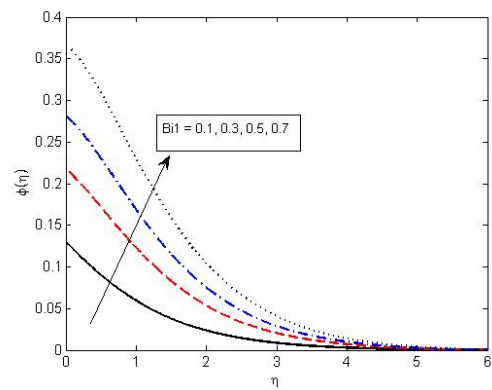


FIGURE 3.12: Influence of thermal Biot number on concentration distribution when $N_t = N_b = Bi_2 = 0.1$ and $Le = M = fw = 1$

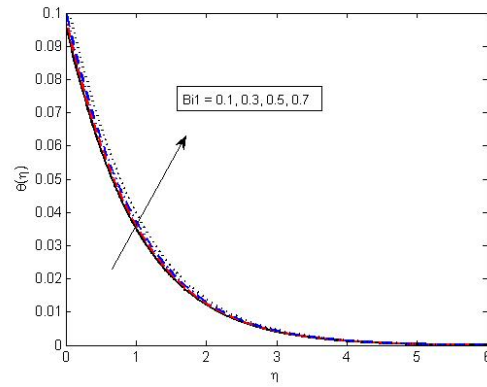


FIGURE 3.13: Influence of concentration Biot number on temperature distribution if $N_t = N_b = Bi_1 = 0.1$ and $Le = M = fw = 1$

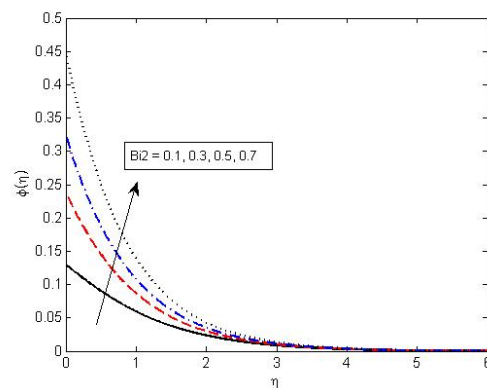


FIGURE 3.14: Influence of concentration Biot number on concentration distribution if $N_t = N_b = Bi_1 = 0.1$ and $Le = M = fw = 1$

Chapter 4

The effect of Joule heating, viscous dissipation and thermal radiation on the flow of MHD nanofluid

In the present chapter, we have extended the study of [31]. We have discussed this phenomena under the affect of viscous dissipation, Joule heating and thermal radiation which are already defined in Chapter 2. Again the governing equation of this model are solved numerically with the help of shooting method. Flow behavior , temperature distribution and concentration distribution within the boundary layer is described through velocity, temperature and concentration profile.

Here we have considered the flow of MHD nanofluid fluid on a stretching surface. The fluid is considered to be incompressible, laminar, and steady. The equation of continuity, equation of momentum and the energy equation describing the given two dimensional flow are given as

$$\frac{\partial u}{\partial x} + \frac{\partial v}{\partial y} = 0 \quad (4.1)$$

$$u \frac{\partial u}{\partial x} + v \frac{\partial u}{\partial y} = \nu \frac{\partial^2 u}{\partial y^2} - \sigma \frac{B_0^2}{\rho} u \quad (4.2)$$

$$\begin{aligned} u \frac{\partial T}{\partial x} + v \frac{\partial T}{\partial y} = & \alpha \left(\frac{\partial^2 T}{\partial y^2} \right) + \tau \left[D_B \left(\frac{\partial C}{\partial y} \frac{\partial T}{\partial y} \right) + \frac{D_T}{T_\infty} \left(\frac{\partial T}{\partial y} \right)^2 \right] + \frac{\nu}{c_f} \left(\frac{\partial u}{\partial y} \right)^2 \\ & + \frac{\sigma B_0^2}{\rho c_f} u^2 - \frac{1}{\rho c_f} \frac{\partial q_r}{\partial y} \end{aligned} \quad (4.3)$$

$$u \frac{\partial C}{\partial x} + v \frac{\partial C}{\partial y} = D_B \left(\frac{\partial^2 C}{\partial y^2} \right) + \frac{D_T}{T_\infty} \left(\frac{\partial^2 C}{\partial y^2} \right) \quad (4.4)$$

Rosseland approximation of radiation gives

$$q_r = -\frac{4\sigma^*}{3\delta} \frac{\partial T^4}{\partial y},$$

where σ^* is Boltzmann constant whose value is 1.38×10^{-23} and δ represents the coefficient of mean absorption, and value of T^4 is given by

$$T^4 = 4T_\infty^3 T - 3T_\infty^4$$

Boundary conditions can be written as

$$u = u_w(x), v = v_x, -K \frac{\partial T}{\partial y} = h_1(T_w - T), -D_B \frac{\partial C}{\partial y} = h_2(C_w - C) \quad \text{at } y = 0, \quad (4.5)$$

$$u \longrightarrow 0, \quad T \longrightarrow T_\infty, C \longrightarrow C_\infty \quad \text{as } y \longrightarrow \infty \quad (4.6)$$

In the above equations, T is temperature of the fluid, T_∞ the surrounding temperature, h_s the heat transfer coefficient, ν the kinematic viscosity and α the thermal diffusivity. The equation of continuity can be justified if a stream function ψ is chosen in a way that

$$u = \frac{\partial \psi}{\partial y} \quad \text{and} \quad v = -\frac{\partial \psi}{\partial x}.$$

Introduce the given similarity transformation,

$$\begin{aligned}\psi &= (av)^{\frac{1}{2}}xf(\eta), & \eta &= \left(\frac{a}{v}\right)^{\frac{1}{2}}y, \\ \theta(\eta) &= \frac{T - T_{\infty}}{T_w - T_{\infty}} \\ \theta(\eta) &= \frac{C - C_{\infty}}{C_w - C_{\infty}}\end{aligned}$$

By introducing the following similarity transformation defined above, equations (4.1) – (4.4) gives

$$f''' + ff'' - (f')^2 - Mf' = 0, \quad (4.7)$$

$$(1 + \frac{4}{3}N)\theta'' + \mathbf{Pr}[f\theta' + Nb\theta'\phi' + Nt(\theta')^2 + E_c f''^2 + E_c M^2 f'^2] = 0 \quad (4.8)$$

$$\phi'' + \mathbf{Le}f\theta' + \frac{Nt}{Nb}\theta'' = 0 \quad (4.9)$$

The associated boundary conditions (4.7) and (4.8) get the form,

$$f(0) = f_w \quad f'(0) = 1, \quad \theta'(0) = -B_{i_{\theta}}(1 - \theta(0)), \quad \phi'(0) = -B_{i_{\phi}}(1 - \phi(0)) \quad (4.10)$$

$$f' \rightarrow 0, \quad \theta \rightarrow 0 \quad \phi \rightarrow 0 \quad \text{as } \eta \rightarrow \infty \quad (4.11)$$

4.1 Numerical solution

In order to solve the above attained ODEs , we will use the shooting method. To solve the above system numerically, we will replace the domain $[0, \infty)$ by the bounded domain $[0, \eta_{\infty}]$ where η_{∞} is some suitable finite real number. Let us use the notation $f = y_1$, $\theta = y_4$, $\phi = y_6$. Further denote $f' = y_1'$ by y_2 , $f'' = y_2'$ by y_3 , θ' by y_5 , $\phi' = y_6'$ by y_7 to have the following system of first order ODEs.

$$y'_1 = y_2 \quad y_1(0) = f_w \quad (4.12)$$

$$y'_2 = y_3 \quad y_2(0) = 1 \quad (4.13)$$

$$y'_3 = y_2^2 + My_2 - y_1y_3 \quad y_3(0) = Y_3 \quad (4.14)$$

$$y'_4 = y_5, \quad y_4(0) = Y_4 \quad (4.15)$$

$$y'_5 = -\frac{\mathbf{Pr}}{1 + \frac{4}{3}N} \left(y_1y_5 + N_b y_5 y_7 + N_t y_7^2 + E_c y_3^2 + E_c M^2 y_2^2 \right), \quad y_5(0) = -B_{i_\theta} (1 - t) \quad (4.16)$$

$$y'_6 = y_7, \quad y_6(0) = Y_6 \quad (4.17)$$

$$y'_7 = -\frac{N_t}{N_b} \left(\frac{\mathbf{Pr}}{1 + \frac{4}{3}N} \right) \left(y_1y_5 + N_b y_5 y_7 + N_t y_7^2 + E_c y_3^2 + E_c M^2 y_2^2 \right) - L_e y_1 y_7, \quad y_7(0) = -B_{i_\phi} (1 - u) \quad (4.18)$$

In the system of equations (4.12) – (4.18), the missing initial conditions Y_3 , Y_4 and Y_6 are to be chosen such that

$$y_2(\eta_\infty, Y_3, Y_4, Y_6) = 0, \quad y_4(\eta_\infty, Y_3, Y_4, Y_6) = 0, \quad y_6(\eta_\infty, Y_3, Y_4, Y_6) = 0. \quad (4.19)$$

To solve the system of algebraic equations (4.19), we use the Newton's method which has the following iterative scheme

$$\begin{pmatrix} Y_3^{(k+1)} \\ Y_4^{(k+1)} \\ Y_6^{(k+1)} \end{pmatrix} = \begin{pmatrix} Y_3^{(k)} \\ Y_4^{(k)} \\ Y_6^{(k)} \end{pmatrix} - \begin{pmatrix} \frac{\partial y_2}{\partial Y_3} & \frac{\partial y_2}{\partial Y_4} & \frac{\partial y_2}{\partial Y_6} \\ \frac{\partial y_4}{\partial Y_3} & \frac{\partial y_4}{\partial Y_4} & \frac{\partial y_4}{\partial Y_6} \\ \frac{\partial y_6}{\partial Y_3} & \frac{\partial y_6}{\partial Y_4} & \frac{\partial y_6}{\partial Y_6} \end{pmatrix}_{(\eta_\infty, Y_3^{(k)}, Y_4^{(k)}, Y_6^{(k)})}^{-1} \begin{pmatrix} y_2^{(k)} \\ y_4^{(k)} \\ y_6^{(k)} \end{pmatrix}_{(Y_3^{(k)}, Y_4^{(k)}, Y_6^{(k)})}$$

Let us now use the following notations:

$$\begin{aligned} \frac{\partial y_1}{\partial Y_3} &= y_8, \quad \frac{\partial y_2}{\partial Y_3} = y_9, \quad \dots \quad \frac{\partial y_7}{\partial Y_3} = y_{14}, \\ \frac{\partial y_1}{\partial Y_4} &= y_{15}, \quad \frac{\partial y_2}{\partial Y_4} = y_{16}, \quad \dots \quad \frac{\partial y_7}{\partial Y_4} = y_{21}, \\ \frac{\partial y_1}{\partial Y_6} &= y_{22}, \quad \frac{\partial y_2}{\partial Y_6} = y_{23}, \quad \dots \quad \frac{\partial y_7}{\partial Y_6} = y_{28}. \end{aligned}$$

With these new notation, the Newton's iterative scheme get the following form.

$$\begin{pmatrix} Y_3^{(k+1)} \\ Y_4^{(k+1)} \\ Y_6^{(k+1)} \end{pmatrix} = \begin{pmatrix} Y_3^{(k)} \\ Y_4^{(k)} \\ Y_6^{(k)} \end{pmatrix} - \begin{pmatrix} y_9 & y_{16} & y_{23} \\ y_{11} & y_{18} & y_{25} \\ y_{13} & y_{20} & y_{27} \end{pmatrix}^{-1}_{(\eta_\infty, Y_3^{(k)}, Y_4^{(k)}, Y_6^{(k)})} \begin{pmatrix} y_2^{(k)} \\ y_4^{(k)} \\ y_6^{(k)} \end{pmatrix}_{(Y_3^{(k)}, Y_4^{(k)}, Y_6^{(k)})} \quad (4.20)$$

For the execution of the above iterative scheme, we differentiate equations (4.12) – (4.18) turn by turn with respect to Y_3, Y_4, Y_6 to have the following IVP consisting of system of twenty one ODEs:

$$y'_8 = y_9, \quad y_8(0) = 0 \quad (4.21)$$

$$y'_9 = y_{10}, \quad y_9(0) = 0 \quad (4.22)$$

$$y'_{10} = 2y_2y_9 + My_9 - [y_8y_3 + y_1y_{10}], \quad y_{10}(0) = 1 \quad (4.23)$$

$$y'_{11} = y_{12}, \quad y_{11}(0) = 0 \quad (4.24)$$

$$y'_{12} = -Pr[y_8y_5 + y_1y_{12} + N_b(y_{12}y_7 + y_5y_{14}) + 2N_t y_7 y_{14}], \quad y_{12}(0) = 0 \quad (4.25)$$

$$y'_{13} = y_{14}, \quad y_{13}(0) = 0 \quad (4.26)$$

$$y'_{14} = \frac{N_t}{N_b} \left(\frac{Pr}{1 + \frac{4N}{3}} \right) \left[(y_8y_5 + y_1y_{12}) + N_b(y_{12}y_7 + y_5y_{14}) + 2N_t y_7 y_{14} \right. \\ \left. + 2E_c y_3 y_{10} + 2E_c M^2 y_2 y_9 \right] - L_e(y_8y_7 + y_1y_{14}), \quad y_{14}(0) = 0 \quad (4.27)$$

$$y'_{15} = y_{16}, \quad y_{15}(0) = 0 \quad (4.28)$$

$$y'_{16} = y_{17}, \quad y_{16}(0) = 0 \quad (4.29)$$

$$y'_{17} = 2y_2y_{16} + My_{16} - [y_{15}y_3 + y_1y_{17}], \quad y_{17}(0) = 0 \quad (4.30)$$

$$y'_{18} = y_{19}, \quad y_{18}(0) = 1 \quad (4.31)$$

$$y'_{19} = -Pr[y_{15}y_5 + y_1y_{19} + N_b(y_{19}y_7 + y_5y_{21}) + 2N_t y_7 y_{21}], \quad y_{19}(0) = -B_{i_0} \quad (4.32)$$

$$y'_{20} = y_{21}, \quad y_{20}(0) = 0 \quad (4.33)$$

$$y'_{21} = \frac{N_t}{N_b} \left(\frac{P_r}{1 + \frac{4N}{3}} \right) \left[(y_{15}y_5 + y_1y_{19}) + N_b(y_{19}y_7 + y_5y_{21}) + 2N_t y_7 y_{21} + 2E_c y_3 y_{17} + 2E_c M^2 y_2 y_{16} \right] - L_e(y_{15}y_7 + y_1y_{21}), \quad y_{21}(0) = 0 \quad (4.34)$$

$$y'_{22} = y_{23}, \quad y_{22}(0) = 0 \quad (4.35)$$

$$y'_{23} = y_{24}, \quad y_{23}(0) = 0 \quad (4.36)$$

$$y'_{24} = 2y_2 y_{23} + M y_{23} - [y_{22} y_3 + y_1 y_{24}], \quad y_{24}(0) = 0 \quad (4.37)$$

$$y'_{25} = y_{26}, \quad y_{25}(0) = 0 \quad (4.38)$$

$$y'_{26} = -P_r [y_{22} y_5 + y_1 y_{26} + N_b(y_{26} y_7 + y_5 y_{28}) + 2N_t y_7 y_{28}], \quad y_{26}(0) = 0 \quad (4.39)$$

$$y'_{27} = y_{28}, \quad y_{27}(0) = 1 \quad (4.40)$$

$$y'_{28} = \frac{N_t}{N_b} \left(\frac{P_r}{1 + \frac{4N}{3}} \right) \left[(y_{22} y_5 + y_1 y_{26}) + N_b(y_{26} y_7 + y_5 y_{28}) + 2N_t y_7 y_{28} + 2E_c y_3 y_{24} + 2E_c M^2 y_2 y_{23} \right] - L_e(y_{22} y_7 + y_1 y_{28}), \quad y_{28}(0) = -B_{i\phi}. \quad (4.41)$$

The above equations are solved using Runge-Kutta method of order 4 with an initial guess $Y_3^{(0)}, Y_4^{(0)}, Y_6^{(0)}$. These guesses are updated by the Newton's method. The iterative process is repeated until the following criteria is met

$$\max(|y_2(\eta_\infty) - |, |y_4(\eta_\infty) - |, |y_6(\eta_\infty) - |) < \epsilon,$$

where $\epsilon > 0$ is the tolerance. For all computation in this chapter, we have fixed $\epsilon = 10^{-8}$.

4.2 Results and discussion

Table 4.1 shows the effect of N and E_c on skin-friction coefficient, Nusselt number and Sherwood number. Increasing the values of N does not affect the skin friction coefficient. By increasing N Nusselt number and Sherwood number also increases. Increasing E_c gives the similar effect.

Figures 4.1, 4.2 and 4.3 show the effect of magnetic parameter on velocity profile, temperature distribution and concentration distribution respectively. It can be seen from the figures that velocity boundary layer thickness decreases with the increase in magnetic parameter whereas temperature and concentration distribution show a little increase

N	Ec	Le	fw	N_t	N_b	B_{i_1}	B_{i_2}	$-f''(0)$	$-\theta'(0)$	$-\phi'(0)$
0.1	1	1	1	0.1	0.1	0.1	0.1	1.231568	0.212301	0.312143
0.3								1.231568	0.223304	0.322146
0.5								1.231568	0.243095	0.332148
0.7								1.231568	0.252312	0.352155
	0.1							1.156671	0.237845	0.317041
	0.3							1.156673	0.247855	0.333045
	0.5							1.156675	0.256859	0.347049
	0.7							1.156679	0.267866	0.350152

TABLE 4.1: Numerical values of $-f''(0)$, $-\theta'(0)$ and $-\phi'(0)$ for different parameters

with the increase in magnetic parameter. It is due to the Lorentz force which is created by applying magnetic field to the conducting fluid. Lorentz force has the tendency to reduce the speed of flow which supports our results. By applying magnetic field on the fluid, the resistance on the fluid particles increases which results in the increase in temperature. Figures 4.4 and 4.5 represent the effect of Brownian motion, parameter and thermophoresis parameter on temperature and concentration profile. An increase in Brownian motion parameter increase the temperature. Similarly increase in thermophoresis parameter increases the concentration distribution. So distribution of nano particles can be adjusted by adjusting Brownian motion parameter. It can also be said that thermophoresis helps in diffusion of nano particles. Figure 4.6 reflects the effect of Lewis number on concentration profile. Lewis number can be defined as the ratio of thermal diffusion to the molecular diffusion. It is convenient of help us find the relation between mass and heat transfer coefficient. By increasing Lewis number the concentration profile become more steeper. Figures 4.7, 4.8 and 4.9 show the effect of suction parameter on velocity profile, temperature distribution and concentration distribution. By increasing the suction parameter a decrease in velocity profile, temperature distribution and concentration distribution is observed. If suction is applied on vertical surface it allows the fluid to draw in the surface which affects the boundary layer thickness. Figures 4.10, 4.11 and 4.12 represent the effect of thermal Biot number and concentration Biot number on temperature and concentration distribution. Increase in thermal and concentration Biot number increases the temperature and concentration distribution. Increase in Biot numbers, increases heat transfer coefficient which increases the temperature. Fig. 4.13, 4.14 and 4.15 shows the effect of thermal radiation on velocity, temperature and concentration profile respectively. By increasing thermal radiation, increase in temperature and concentration profile is observed. Fig 4.16 and 4.17 shows

the effect of viscous dissipation on temperature and concentration profile. It is observed that increase in dissipation also increases temperature and concentration profile. Table 4.1 gives the values of temperature and concentration profile for different parameters described.

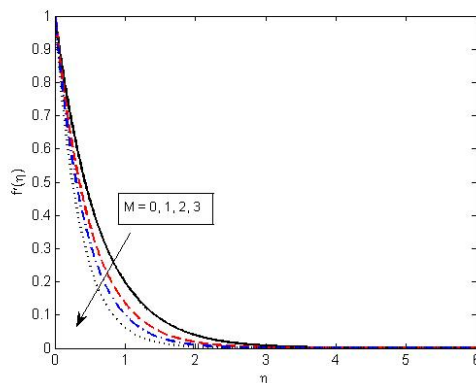


FIGURE 4.1: Influence of magnetic parameter on velocity profile if $E_c = N = N_b = N_t = Bi_1 = Bi_2 = 0.1$ and $Le = fw = 1$

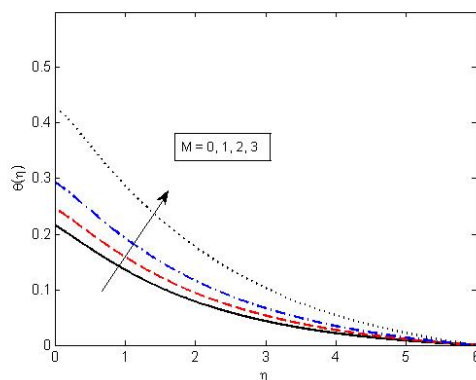


FIGURE 4.2: Influence of magnetic parameter on temperature distribution if $N = E_c = N_b = N_t = Bi_1 = Bi_2 = 0.1$ and $Le = fw = 1$

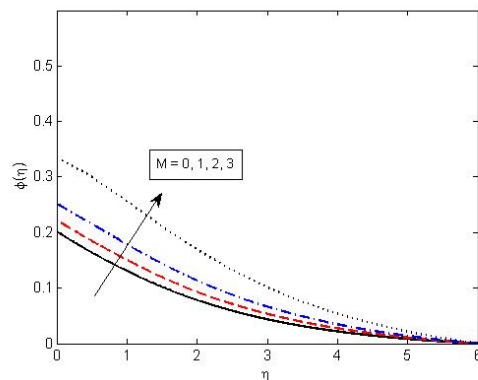


FIGURE 4.3: Influence of magnetic parameter concentration distribution if $N = E_c = N_b = N_t = Bi_1 = Bi_2 = 0.1$ and $Le = fw = 1$

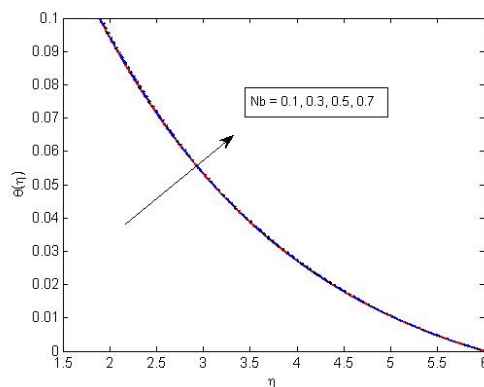


FIGURE 4.4: Influence of Brownian motion parameter on temperature distribution if $N = E_c = N_t = Bi_1 = Bi_2 = 0.1$ and $M = Le = fw = 1$

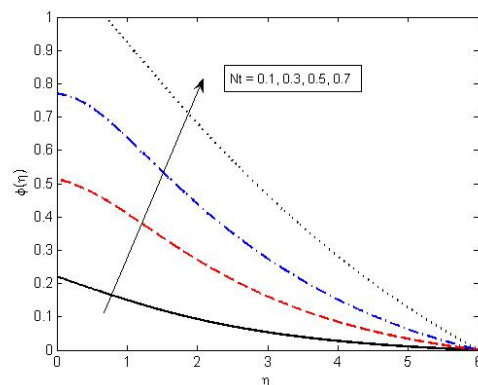


FIGURE 4.5: Influence of thermophoresis parameter on concentration distribution if $N = E_c = N_b = Bi_1 = Bi_2 = 0.1$ and $M = Le = fw = 1$

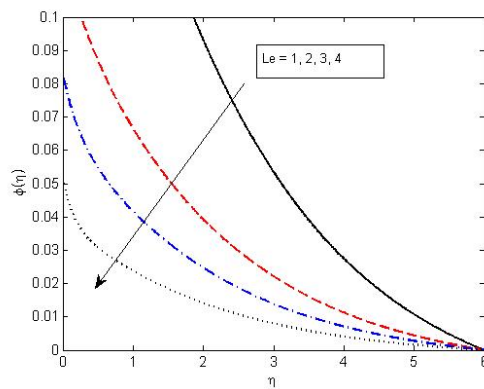


FIGURE 4.6: Influence of Lewis number on concentration distribution if $N = E_c = N_t = N_b = Bi_1 = Bi_2 = 0.1$ and $M = fw = 1$

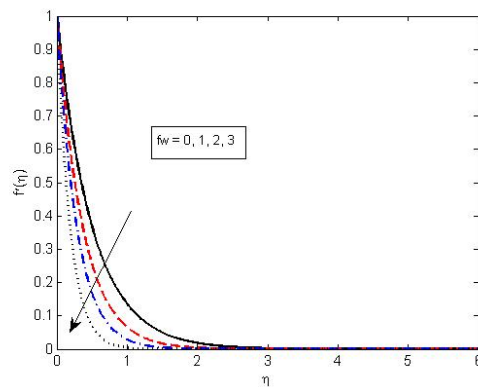


FIGURE 4.7: Influence of suction parameter on velocity profile if $N_t = N_b = Bi_1 = Bi_2 = 0.1$ and $M = Le = 1$

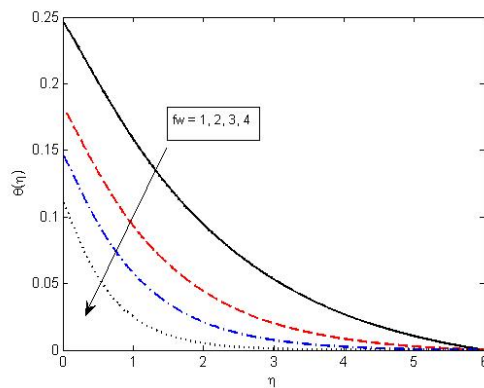


FIGURE 4.8: Influence of suction parameter on temperature distribution if $N_t = N_b = Bi_1 = Bi_2 = 0.1$ and $M = Le = 1$

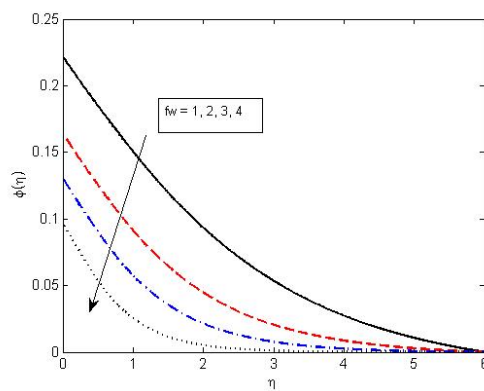


FIGURE 4.9: Influence of suction parameter on concentration distribution if $N_t = N_b = Bi_1 = Bi_2 = 0.1$ and $M = Le = 1$

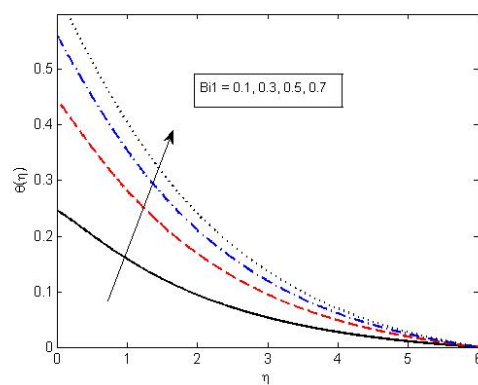


FIGURE 4.10: Influence of thermal Biot number on temperature distribution if $N_t = N_b = Bi_2 = 0.1$ and $M = Le = fw = 1$

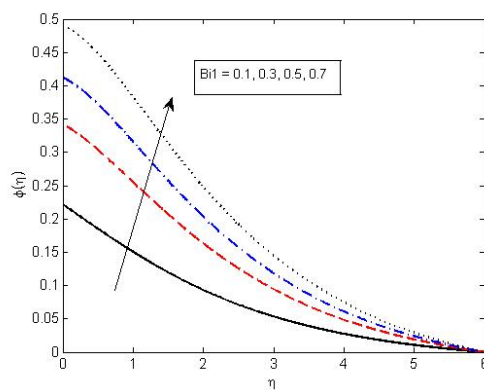


FIGURE 4.11: Influence of thermal Biot number on concentration distribution if $N_t = N_b = Bi_2 = 0.1$ and $M = Le = fw = 1$

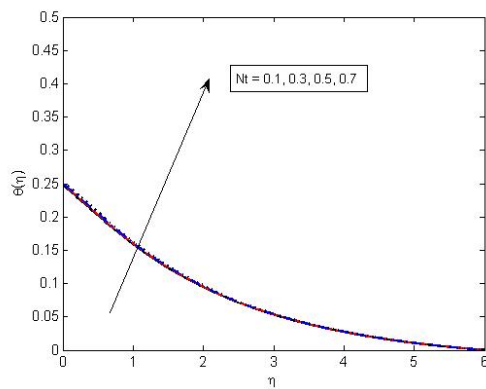


FIGURE 4.12: Effect of concentration Biot number on temperature distribution when $N_t = N_b = Bi_1 = 0.1$ and $M = Le = fw = 1$

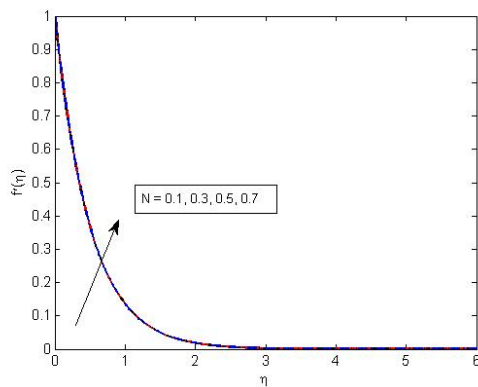


FIGURE 4.13: Effect of thermal radiation on velocity profile when $N_b = N_t = Bi_1 = Bi_2 = 0.1$ and $Le = fw = 1$

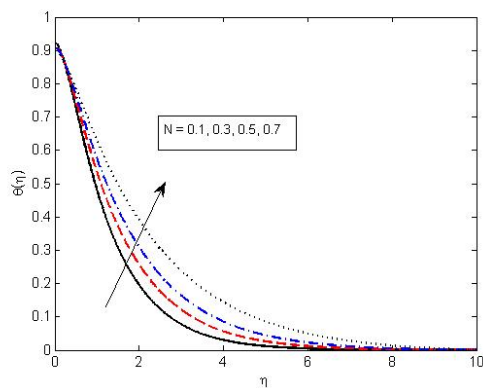


FIGURE 4.14: Effect of thermal radiation on temperature profile when $N_b = N_t = Bi_1 = Bi_2 = 0.1$ and $Le = fw = 1$

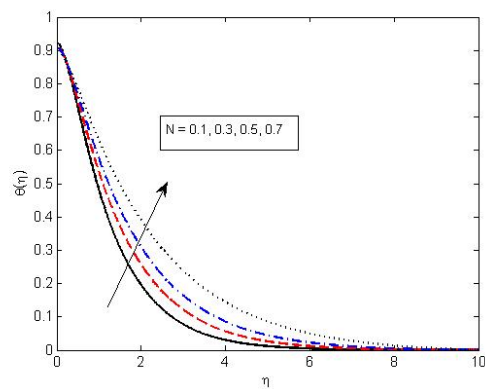


FIGURE 4.15: Effect of thermal radiation on concentration profile when $N_b = N_t = Bi_1 = Bi_2 = 0.1$ and $Le = fw = 1$

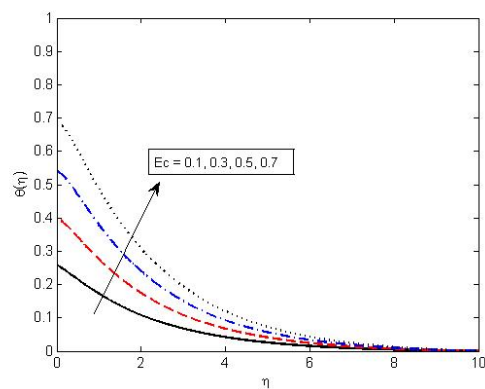


FIGURE 4.16: Effect of viscous dissipation on temperature profile when $N_b = N_t = Bi_1 = Bi_2 = 0.1$ and $Le = fw = N = 1$

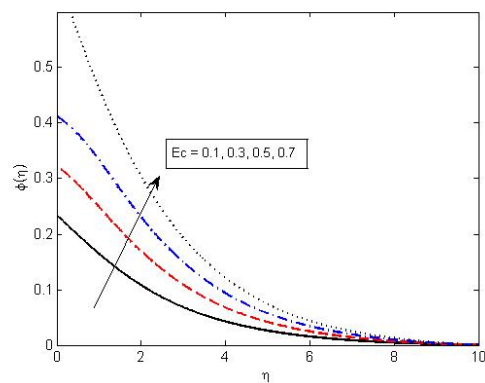


FIGURE 4.17: Effect of viscous dissipation on concentration profile when $N_b = N_t = Bi_1 = Bi_2 = 0.1$ and $Le = fw = N = 1$

4.3 Conclusion

In this dissertation, the behaviour of flow of MHD Nanofluid on a stretching sheet due to convective boundary conditions at the boundary layer is discussed. The obtained equations of the problem are converted into ODE's using similarity transformation. By the help of shooting method, the solution of given problem is obtained numerically and the following results are observed:

- (i) Increase in magnetic parameter decreases boundary layer thickness whereas increases temperature and concentration profile.
- (ii) Increase in Brownian motion parameter increases temperature.
- (iii) Increase in thermophoresis parameter increases concentration profile.
- (iv) Increase in suction parameter decreases velocity, temperature and concentration profile.
- (v) Increase in thermal and concentration Biot number increases temperature and concentration profile.
- (vi) Increase in thermal radiation increases temperature and concentration profile.
- (vii) Increase in viscous dissipation increases temperature and concentration profile.

Bibliography

- [1] L. J. Crane, Flow past a stretching plate, *Z.A.M.P.*, 21, pp. 645-647. (1970)
- [2] S. Mukhopadhyay, Heat transfer analysis of unsteady flow of a Maxwell fluid over a stretching surface in the presence of a heat source/sink, *Chinese Phys. Lett.*, 29, pp. 054703. (2012)
- [3] B. Sahoo, Effects of slip on sheet-driven flow and heat transfer of a non-Newtonian fluid past a stretching sheet, *Compt. Math. Appl.*, 61, pp. 14421456. (2011)
- [4] M. M. Rashidi, A.J. Chamkha, M. Keimanesh, Application of Multi-step differential transform method on flow of a second grade fluid over a stretching or shrinking sheet, *Amer. J. Compt. Math*, 6, pp.119128. (2011)
- [5] M. Ramzan, M. Farooq, A. Alsaedi, T. Hayat, MHD three-dimensional flow of couple stress fluid with Newtonian heating, *Eur. Phys. J. Plus*, 128, pp. 49-56. (2013)
- [6] S. U. S. Choi, Enhancing thermal conductivity of fluids with nanoparticles, D. A. Siginer, H.P. Wang (Eds.), *Developments and applications of non-Newtonian flows*, ASME FED, 66, pp. 99105. (1995)
- [7] J. Bouniorno, A benchmark study of thermal conductivity of nanofluids, *J. Appl. Phys.*, 106, pp. 094312. (2009)
- [8] K. Khanafer, K. Vafai, M. Lightstone, Buoyancy-driven heat transfer enhancement in a two-dimensional enclosure utilizing nanofluids, *Int. J. heat Mass transf.*, 46, pp. 3639-3653. (2003)
- [9] M. Sheikholeslami, H. R. Ashorynejad, D. D. Ganji, A. Kolahdooz, Investigation of rotating MHD viscous flow and heat transfer between stretching and porous surfaces using analytical method, *Math Probl. Eng.*, (2011)
- [10] R. Ellahi, M. Hameed, Numerical analysis of steady flows with heat transfer, MHD and nonlinear slip effects, *Int. J. Numer. Methds. Heat Fluid Flow*, 22 (1), pp. 2438.(2012)

- [11] O. D. Makinde, W. A. Khan, Z. H. Khan, Buoyancy effects on MHD stagnation point flow and heat transfer of a nanofluid past a convectively heated stretching/shrinking sheet, *Int. J. Heat Mass Transf.*, 62, pp. 526533. (2013)
- [12] S. Nadeem, R. Mehmood, N. S. Akbar, Thermo-diffusion effects on MHD oblique stagnation-point flow of a viscoelastic fluid over a convective surface, *Eur. Phys. J. Plus*, 129, pp. 118. (2014)
- [13] W. A. Khan, O. D. Makinde, Z. H. Khan, MHD boundary layer flow of a nanofluid containing gyrotactic microorganisms past a vertical plate with Navier slip, *Int. J. Heat Mass Transf.*, 74, pp. 285291. (2014)
- [14] N. Vishnu Ganesh, B. Ganga, A. K. Abdul Hakeem, Lie symmetry group analysis of magnetic field effects on free convective flow of a nanofluid over a semi infinite stretching sheet, *J. Egypt. Math Soc.*, 22, pp. 304310. (2014)
- [15] N. Vishnu Ganesh, A. K. Abdul Hakeem, R. Jayaprakash, B. Ganga, Analytical and numerical studies on hydromagnetic flow of water based metal nanofluids over a stretching sheet with thermal radiation effect, *J. Nanofluids.*, 3, pp. 154161. (2014)
- [16] M. M. Rashidi, N. Vishnu Ganesh, A. K. Abdul Hakeem, B. Ganga, Buoyancy effect on MHD flow of nanofluid over a stretching sheet in the presence of thermal radiation, *J. Mol. liq.*, 198, pp. 234238. (2014)
- [17] W. Ibrahim, O. D. Makinde, Double-diffusive in mixed convection and MHD stagnation point flow of nanofluid over a stretching sheet, *J. Nanofluids*, 4, pp. 2837. (2015)
- [18] S. Das, H. K. Mandal, R. N. Jana, O.D. Makinde, Magneto-nanofluid flow past an impulsively started porous flat plate in a rotating frame, *J. Nanofluids*, 4, pp. 167175. (2015)
- [19] S. Nadeem, Rashid Mehmood, S. S. Motsa, Numerical investigation on MHD oblique flow of a Walters B type nanofluid over a convective surface, *Int. J. Therm. Sci.*, 92, pp. 162172. (2015)

- [20] S. Nadeem, R. Mehmood, N. S. Akbar, Combined effects of magnetic field and partial slip on obliquely striking rheological fluid over a stretching surface, *J. Magn. Mater.*, 378, pp. 457462. (2015)
- [21] A. K. Abdul Hakeem, N. Vishnu Ganesh, B. Ganga, Magnetic field effect on second order slip flow of nanofluid over a stretching/shrinking sheet with thermal radiation effect, *J. Magn. Mater.*, 381, pp. 243257. (2015)
- [22] P. O. Olanrewaju, M. A. Olanrewaju, Adesanya, Boundary layer flow of nanofluids over a moving surface in a flowing fluid in the presence of radiation, *Int. J. Appl. Sci. Technol.*, 2, pp. 274285. (2012)
- [23] T. Poornima, N. Bhaskar Reddy, Radiation effects on MHD free convective boundary layer flow of nanofluids over a nonlinear stretching sheet, *Adv. Appl. Sci. Res.*, 4, pp. 190202. (2013)
- [24] M. Turkyilmazoglu, I. Pop, Heat and mass transfer of unsteady natural convection flow of some nanofluids past a vertical infinite flat plate with radiation effect, *Int. J. Therm. Sci.*, 59, pp. 167171. (2013)
- [25] S. P. Anjali Devi, B. Ganga, Effects of viscous and Joules dissipation on MHD flow, heat and mass transfer past a stretching porous surface embedded in a porous medium, *Nonlinear Anal. Model Control*, 14, pp. 303314. (2009)
- [26] T. G. Motsumi, O. D. Makinde, Effects of thermal radiation and viscous dissipation on boundary layer flow of nanofluids over a permeable moving flat plate, *Phys. Scr.*, 86, pp. 045003. (2012)
- [27] O. D. Makinde, W. N. Mutuku, Hydromagnetic thermal boundary layer of nanofluids over a convectively heated flat plate with viscous dissipation and Ohmic heating, *UPB Sci. Bull. Ser. A*, 76, pp. 181192. (2014)
- [28] S. E. Ahmed, A. K. Hussein, H. A. Mohammed, S. Sivasankaran, Boundary layer flow and heat transfer due to permeable stretching tube in the presence of heat source/sink utilizing nanofluids, *Appl. Math Comput.*, 238, pp. 149162. (2014)

-
- [29] S. Akilu, M. Narahari, Effects of heat generation or absorption on free convection flow of a nanofluid past an isothermal inclined plate, *Adv. Mater. Res.*, 970, pp. 267271. (2014)
- [30] R. Viskanta, R.J. Grosh, Boundary layer in thermal radiation absorbing and emitting media, *Int. J. Heat. Mass Transf.*, 5, pp. 795-806. (1962)
- [31] H. Ajam, Analytical approximation of MHD nanofluid flow induced by a stretching permeable surface using Buongiorno's model, 3, pp. 3-9. (2016)
- [32] F. K. Tsou, E.M. Sparrow, R.J. Goldstein, Flow and heat transfer in the boundary layer on a continuous moving surface, *Int. J. Heat Mass Transf.*, 10, pp. 219-235. (1967)
- [33] L. E. Erickson , Fan LT, Fox VG Heat and mass transfer in the laminar boundary layer flow of a moving flat surface with constant surface velocity and temperature focusing on the effects of suction/injection, *Ind. Eng. Chem.*, 5, pp. 19-25. (1966)
- [34] M. M. Nandeppanavar, Vajravelu K, Abel MS, Heat transfer in MHD viscoelastic boundary layer flow over a stretching sheet with thermal radiation and non-uniform heat source/sink, *Commun. Nonlinear Sci. Numer. Simulat.*, 16, pp.3578-3590. (2011)
- [35] A. Van Deynse, P. Cools, C. Leys, N. De Geyter, R. Morent, Surface activation of polyethylene with an argon atmospheric pressure plasma jet: Influence of applied power and flow rate, *Appl. Sur. Sci.*, 328 (15), pp. 269-278. (2015)